

Methods for Correction of the Single-Nucleotide Substitution c.840C>T in Exon 7 of the *SMN2* Gene

K. R. Valetdinova^{1,2,3,4,a*}, V. S. Ovechkina^{1,2,3,4}, and S. M. Zakian^{1,2,3,4}

¹Federal Research Center Institute of Cytology and Genetics, Siberian Branch of the Russian Academy of Sciences, 630090 Novosibirsk, Russia

²Institute of Chemical Biology and Fundamental Medicine, Siberian Branch of the Russian Academy of Sciences, 630090 Novosibirsk, Russia

³Meshalkin National Medical Research Centre, Ministry of Healthcare of Russian Federation, 630090 Novosibirsk, Russia

⁴Novosibirsk State University, 630090 Novosibirsk, Russia

^ae-mail: valetdinova@bionet.nsc.ru

Received April 30, 2019

Revised June 3, 2019

Accepted June 3, 2019

Abstract—The CRISPR/Cas technology has a great potential in the treatment of many hereditary diseases. One of the prospective models for the CRISPR/Cas-mediated therapy is spinal muscular atrophy (SMA), a disease caused by deletion of the *SMN1* gene that encodes the SMN protein required for the survival of motor neurons. SMA patients' genomes contain either single or several copies of *SMN2* gene, which is a paralog of *SMN1*. Exon 7 of *SMN2* has the single-nucleotide substitution c.840C>T leading to the defective splicing and decrease in the amounts of the full-length SMN. The objective of this study was to create and test gene-editing systems for correction of the single-nucleotide substitution c.840C>T in exon 7 of the *SMN2* gene in fibroblasts, induced pluripotent stem cells, and motor neuron progenitors derived from a SMA patient. For this purpose, we used plasmid vectors expressing CRISPR/Cas9 and CRISPR/Cpf1, plasmid donor, and 90-nt single-stranded oligonucleotide templates that were delivered to the target cells by electroporation. Although sgRNA_T2 and sgRNA_T3 guiding RNAs were more efficient than sgRNA_T1 in fibroblasts ($p < 0.05$), no significant differences in the editing efficiency of sgRNA_T1, sgRNA_T2, and sgRNA_T3 was observed in patient-specific induced pluripotent stem cells and motor neuron progenitors. The highest editing efficiency in induced pluripotent stem cells and motor neuron progenitors was demonstrated by the sgRNA_T1 and 90-nt single-stranded oligonucleotide donors.

DOI: 10.1134/S0006297919090104

Keywords: spinal muscular atrophy, induced pluripotent stem cells, motor neuron progenitors, gene editing

One of the approaches for the treatment of hereditary diseases is correction of mutations in induced pluripotent stem cells (iPSCs) derived from the patient's somatic cells or regional stem cells using modern gene-editing systems with subsequent autologous transplantation of "corrected" progenitor cells or their differentiated derivatives into the patient's body. Currently, CRISPR Therapeutics and Vertex Pharmaceuticals (USA) are conducting phase I/II clinical trials of a similar *ex vivo* therapy for β -thalassemia and sickle cell anemia and are expected to start analogous trials for Duchenne muscular

dystrophy and some other diseases. However, the question whether a CRISPR-mediated system will be efficient in the treatment of hereditary diseases of the central nervous system remains open. Spinal muscular atrophy (SMA) occupies a special place among such diseases. SMA is one of the most common hereditary diseases that develop in childhood and one of the main causes of early infant mortality. The most severe form of this disease, SMA type I, develops during the first months of life and leads to the patient's death within two years [1]. In 95% cases, SMA is caused by a homozygous deletion of the *SMN1* gene coding for the SMN protein that controls various aspects of RNA metabolism [2]. SMN is also synthesized from the *SMN2* gene, a highly homologous copy of *SMN1*. Therefore, SMA patients present a unique situation: *SMN1* gene is deleted or damaged by mutation;

Abbreviations: iPSCs, induced pluripotent stem cells; MNP, motor neuron progenitor; SMA, spinal muscular atrophy; sgRNA, single guide RNA.

* To whom correspondence should be addressed.

however, the paralogous *SMN2* gene, which is almost identical to *SMN1* in its nucleotide sequence, is present in the genome. The difference between these two genes comes to several single-nucleotide substitutions. One of them, c.840C>T, is located in exon 7 and results in the loss of exon 7 in most (~90%) mature *SMN2* transcripts that are translated with a formation of truncated unstable protein unable to support its functions [3]. There are two hypotheses explaining the disruption mechanism. The first one suggests that mutation in the *SMN2* exon 7 disrupts the sequence of the exon splicing enhancer; as a result, the splicing factors do not recognize and bind to the splicing sites, and exon 7 is not included in the mature mRNA [4]. The second hypothesis suggests that the exon splicing silencer is formed, which prevents exon 7 inclusion in the mature mRNA [5]. Due to the instability of this region, the number of *SMN2* copies can vary considerably. The more copies of *SMN2* are in the genome, the more full-length protein is synthesized, and therefore, the less are manifestations of disease symptoms. It was shown that the number of *SMN2* copies correlates with the severity of SMA [6]. Most patients with SMA type I have two *SMN2* copies, patients with SMA type II have three or four *SMN2* copies, and patients with SMA type III have three or four *SMN2* copies. Healthy donors have 1-2 copies of *SMN2* on average.

Despite a large body of data on the pathogenesis and molecular genetics of SMA obtained during the last ten years, the pathogenetic therapy of SMA appeared relatively recently. In 2017, the first treatment for SMA, an antisense oligonucleotide modulating *SMN2* splicing, was approved in the USA and EU [7]. However, the desired therapeutic effect requires regular intrathecal injections of the preparation because of its degradation by the cellular systems over time. Furthermore, the drug provides only a relief of disease symptoms and some increase in the patients' life expectancy, and the long-term effects of treatment have not been studied. The only approach to the etiotropic therapy of SMA today is correction of the c.840C>T substitution in the paralogous gene.

The purpose of this study was to create and test CRISPR-mediated systems for the correction of the single-nucleotide substitution c.840C>T in the *SMN2* exon 7 in fibroblasts, induced pluripotent stem cells (iPSCs), and motor neuron progenitors. First, we had to introduce a double-strand break in the immediate vicinity of the substitution, since for efficient recombination, the distance between the DNA break and the region in which the target substitution is located should not exceed 20 nucleotides [8]. For this purpose, single guide RNAs (sgRNAs) for the CRISPR/Cas9 and CRISPR/Cpf1 systems were selected that introduced double-strand breaks as close as possible to the target substitution in order to increase the frequency of homologous recombination. Donor templates, including plasmid vector with a selection cassette and short single-stranded oligonucleotides, were also designed.

MATERIALS AND METHODS

Plasmid design. Plasmid vectors pX552_miCMV_Puro_SMN, pUC19_SMN2_contr, and pUC19_SMN2_mut were designed using the SnapGene software. DNA fragments amplified from the *SMN1* and *SMN2* genes, fragment 615-818 from the pcDNA 3.1(-) plasmid (Invitrogen, USA), and fragment 6775-7374 from the w-159-1 plasmid (Addgene plasmid #17481; kindly provided by Drs. E. Campeau and P. Kaufman) were used for the assembly. Plasmids pSpCas9(BB)-2A-GFP (pX458) and pY010 (Addgene plasmid #48138 and #69982, respectively) were a gift from Dr. F. Zhang; pTE4560 (Addgene plasmid #107526) was a gift from Dr. E. Welker. Amplification of DNA fragments was performed with Phusion Hot Start II polymerase (Thermo Fisher Scientific, USA) in a C1000 Touch Thermal Cycler (Bio-Rad, USA); the primers are listed in Table 1. Plasmid assembly was performed using standard molecular cloning methods and the Golden Gate technology (NEB, USA). Plasmid clones were sequenced with an ABI 3130XL Genetic Analyzer (Applied Biosystems, USA) at the Genomics Core Facility, Siberian Branch of the Russian Academy of Sciences. Plasmid DNA was isolated using PureLink High Pure Plasmid Midiprep kit (Invitrogen).

Guide RNA and donor design. sgRNAs and donor sequences were designed using the online resource <http://benchling.com>.

Cell culture. We used f1SMA fibroblasts and two iPSC lines (ICGi005-A and ICGi005-B) from a patient with SMA type I [9]. Fibroblasts were cultured in DMEM/F-12 with 10% FBS, 0.1 mM non-essential amino acids (NEAA), 1 mM GlutaMax, 100× penicillin/streptomycin (all Gibco, USA). The cells were split at 1 : 3 every five days using TrypLE (Gibco). iPSCs were cultured in KnockOut DMEM with 15% KnockOut Serum Replacement, 0.1 mM NEAA, 1 mM GlutaMax, 100× penicillin/streptomycin (all Gibco), 0.25 mM 2-mercapthoethanol (Sigma, USA) and 10 ng/ml basic fibroblast growth factor (BioLegend, USA). iPSCs were split at 1 : 10 twice a week using TrypLE.

iPSC differentiation into motor neuron progenitors (MNPs). Differentiation of iPSCs into MNPs was carried out according to the protocol of Du et al. [10]. The cells were dissociated with Accutase (Gibco) and split at (1 : 3)-(1 : 4) twice a week.

Transfection of fibroblasts, iPSCs, and MNPs. iPSCs and fibroblasts were transfected with a Neon Transfection System (Thermo Fisher Scientific) according to the manufacturer's instructions; 5 µg of plasmid DNA or 3 µg of plasmid DNA and 2 µl of 100 µM oligonucleotide donor were mixed with 5·10⁵ cells.

Cell sorting. Cell sorting was performed with a S3e Cell Sorter (Bio-Rad) 48 h after transfection.

DNA isolation and PCR. Genomic DNA was isolated with a Quick-DNA Miniprep Kit (Zymo Research,

Table 1. Primers used in the study

Primer	Gene	5'→3' sequence, application
GA_F2	<i>SMN2</i>	AAGTGATTCTCCTGCCTCAACC knock-in evaluation, TIDE, TIDER
GA_R1	<i>SMN2</i>	CACAACCAACCAGTTAAGTATGAG knock-in evaluation, TIDE, TIDER
NT1_F	<i>LOC105376917</i>	TAGGTAACACAAAGCTCATCCC off-target effect evaluation with TIDE
NT1_R	<i>LOC105376917</i>	AGAGAAGCCAGTTCCTCTA off-target effect evaluation with TIDE
NT5_F	<i>LOC105369801</i>	GCCAGTATACTAGATGGCCTAGA off-target effect evaluation with TIDE
NT5_R	<i>LOC105369801</i>	TCCTTCAGCCTGGTCCTAAA off-target effect evaluation with TIDE
NT2_F	<i>PRPS2</i>	GGTACAGGTGATCTCTCCTTTG off-target effect evaluation with TIDE
NT2_R	<i>PRPS2</i>	GCACAGTAACCAAGATGGTTTATC off-target effect evaluation with TIDE
NT3_F	<i>FANCD2</i>	CAGCCTGCTGTTTGTTCAG off-target effect evaluation with TIDE
NT3_R	<i>FANCD2</i>	GGAAACTGCCTAGAGGTAGAAG off-target effect evaluation with TIDE
NT4_F	<i>FANCD2P2</i>	CTATGTCCCTCCTCTTGAAAC off-target effect evaluation with TIDE
NT4_R	<i>FANCD2P2</i>	TGCTTAGCAGTAGAAGAGGTAAT off-target effect evaluation with TIDE
NT6_F	<i>LIN28B</i>	CCCTTAAGGATACGAGGTGAAA off-target effect evaluation with TIDE
NT6_R	<i>LIN28B</i>	GGGAGGTAATGCCAGTATT off-target effect evaluation with TIDE
GA_Hind_F	<i>SMN2</i>	CCTAAGCTTAAGTATTCTCCTGCCTCAACC cloning <i>SMN2</i> into pUC19_ <i>SMN2</i> _contr
GA_Xba_R	<i>SMN2</i>	GTTTC-TAGAC-ACAAC-CAACC-AGTTA-AGTAT-GAG cloning <i>SMN2</i> into pUC19_ <i>SMN2</i> _contr
BsmBI_F	<i>SMN2</i>	TATCGTCTCTACAGGGTTTCAGACAAAAT introducing T>C substitution into pUC19_ <i>SMN2</i> _mut
BsmBI_R	<i>SMN2</i>	GTCCGTCTCCCTGTAAGGAAAATAAAG introducing T>C substitution into pUC19_ <i>SMN2</i> _mut
AflII_F	<i>SMN2</i>	GCCCTTAAGGTTAATGTAAAAC cloning 3'-homology arm into pX552_miCMV_Puro_ <i>SMN</i>
HindIII_R	<i>SMN2</i>	GCCAAGCTTCCATTCCACTTCCT cloning 3'-homology arm into pX552_miCMV_Puro_ <i>SMN</i>
PciI_ <i>SMN1</i>	<i>SMN2</i>	GCCACATGTTTAAATTTTTGTAGAGAC cloning 5'-homology arm into pX552_miCMV_Puro_ <i>SMN</i>

Table 1 (Contd.)

Primer	Gene	5'→3' sequence, application
AgeI_SMN1	<i>SMN2</i>	CATACCGGTTTTTTTAAATGTTCAAAAAC cloning 5'-homology arm into pX552_miCMV_Puro_SMN
BbsI_Lys_Gln_F	<i>SMN2</i>	ACAGAAGACCAGACAAAATCAAAAGGAAGG introducing synonymous substitutions into pX552_miCMV_Puro_SMN for sgRNA_T2
BbsI_Lys_Gln_R	<i>SMN2</i>	CTTGAAGACTTTGTCTGAAACCCGTGAAGGAAAATAAAG introducing synonymous substitutions into pX552_miCMV_Puro_SMN for sgRNA_T2
NheI_PuroR_F	<i>PuroR</i>	CAGGCTAGCATGACCGAGTAC cloning puromycin resistance gene into pX552_miCMV_Puro_SMN
PuroR_R_KpnI	<i>PuroR</i>	GGGGGTACCTCAGGCACCGG cloning puromycin resistance gene into pX552_miCMV_Puro_SMN
miCMV_PacI	–	GGCTTAATTAAGCGATCTGACG cloning miCMV into pX552_miCMV_Puro_SMN
PacI_miCMV	–	GGCTTAATTAACGGTTTGACTC cloning miCMV into pX552_miCMV_Puro_SMN
Cpf10_S	<i>SMN2</i>	AGATGGACAAAATCAAAAAGAAGGAAGGT cloning sgRNA_T6 into pTE4560
Cpf10_AS	<i>SMN2</i>	AAAAACCTTCCTTCTTTTTGATTTGTCC cloning sgRNA_T6 into pTE4560
Cpf7_S	<i>SMN2</i>	AGATGCCTTACAGGGTTTTAGACAAAATC cloning sgRNA_T5 into pTE4560
Cpf7_AS	<i>SMN2</i>	AAAAGATTTTGTCTAAAACCCTGTAAGGC cloning sgRNA_T5 into pTE4560
Cpf2_S	<i>SMN2</i>	AGATGGTCTAAAACCCTGTAAGGAAAATA cloning sgRNA_T4 into pTE4560
Cpf2_AS	<i>SMN2</i>	AAAATATTTTCCTTACAGGGTTTTAGACC cloning sgRNA_T4 into pTE4560
SMN2_T1_1	<i>SMN2</i>	CACCGATTTTGTCTAAAACCCTGTA cloning sgRNA_T1 into pX458
SMN2_T1_2	<i>SMN2</i>	AAACTACAGGGTTTTAGACAAAATC cloning sgRNA_T1 into pX458
SMN2_T2_1	<i>SMN2</i>	CACCGTTTAGACAAAATCAAAAAGA cloning sgRNA_T2 into pX458
SMN2_T2_2	<i>SMN2</i>	AAACTCTTTTTGATTTTGTCTAAAC cloning sgRNA_T2 into pX458
SMN2_T3_1	<i>SMN2</i>	CACCGGACAAAATCAAAAAGAAGGA cloning sgRNA_T3 into pX458
SMN2_T3_2	<i>SMN2</i>	AAACTCCTTCTTTTTGATTTTGTCC cloning sgRNA_T3 into pX458
GAPDH_S	<i>GAPDH</i>	CGCCAGCCGAGCCACATC qRT-PCR
GAPDH_AS	<i>GAPDH</i>	CGCCCAATACGACCAAATCC-G qRT-PCR

Table 1 (Contd.)

Primer	Gene	5'→3' sequence, application
NANOG_S	<i>NANOG</i>	ATGGAGGAAGGAAGAGGAGA qRT-PCR
NANOG_AS	<i>NANOG</i>	GATTTGTGGGCCTGAAGAAA qRT-PCR
PAX6_RT_F	<i>PAX6</i>	TCCGTTGGAAGTATGGAGT qRT-PCR
PAX6_RT_R	<i>PAX6</i>	GTTGGTATCCGGGGACTTC qRT-PCR
OLIG2_RT_F	<i>OLIG2</i>	GATAGTCGTCGCAGCTTTCG qRT-PCR
OLIG2_RT_R	<i>OLIG2</i>	CCTGAGGCTTTTCGGAGC qRT-PCR

USA). PCR products were purified with a Zymoclean Gel DNA Recovery Kit (Zymo Research). DNA fragments were amplified using a BioMaster HS-Taq PCR-Color 2× kit (Biolabmix, Russia) with a C1000 Touch Thermal Cycler. PCR conditions were: 95°C for 5 min, 35 cycles of 95°C for 30 s, 59°C for 30 s, 72°C for 30 s; then 72°C for 5 min. The primers are listed in Table 1.

RNA extraction and reverse transcription-quantitative PCR (RT-qPCR). RNA was isolated from the cells using TRIzol Reagent (Thermo Fisher Scientific) according to the manufacturer's instructions. cDNA was synthesized with Super Script III Reverse Transcriptase (Thermo Fisher Scientific). qPCR was performed using BioMaster HS-qPCR SYBR Blue 2× (Biolabmix) in a LightCycler 480 system (Roche, Germany). PCR conditions were: 40 cycles of 95°C for 15 s, 60°C for 1 min. The C_T values were normalized to *GAPDH* expression using the $\Delta\Delta CT$ method.

Immunocytochemistry. Immunofluorescent staining was performed according to the following protocol: fixation in 4% formaldehyde (Sigma) for 15 min at room temperature, permeabilization in 0.5% Triton X-100 (Sigma) for 30 min at room temperature, blocking in 1% BSA (Sigma) for 30 min. Incubation was carried out with primary anti-OLIG2 antibodies (AB9610, 1 : 500) (EMD Millipore, USA) for 16 h at 4°C and then with secondary antibodies Alexa Fluor 568 goat anti-rabbit IgG (H+L) (1 : 400; A11011, Thermo Fisher Scientific) for 1.5–2 h at room temperature. 4',6-Diamidino-2-phenylindole dihydrochloride (DAPI) (Sigma) was used for nuclear staining. The images were analyzed with a NIS-Elements Eclipse Ti-E fluorescence microscope (Nikon, Japan).

Analysis of target and off-target activities of the CRISPR systems. CRISPR-mediated editing of target and off-target sites was evaluated using TIDE (for inser-

tions/deletions) and TIDER (for the c.840C>T substitution) tools.

Statistical analysis. Statistical processing of the obtained data was carried out using the Wilcoxon test and ANOVA with the STATISTICA 10.0 software; $p < 0.05$ was considered as statistically significant.

RESULTS

Tool design. Based on the bioinformatic analysis of the *SMN2* gene intron 6 and exon 7 sequences, three protospacers for CRISPR/Cas9 (sgRNA_T1, sgRNA_T2, sgRNA_T3) and three protospacers for CRISPR/Cpf1 (sgRNA_T4, sgRNA_T5, sgRNA_T6) were selected, all of them located within a 20-nt distance from the c.840C>T substitution in exon 7 of *SMN2* gene (Fig. 1). This choice was dictated by the fact that CRISPR/Cas9 introduces double-strand breaks with blunt ends, while CRISPR/Cpf1 cuts DNA with the formation of sticky ends. Therefore, the recombination efficiency of different types of DNA breaks may differ. In addition, the selected protospacers were complementary to different DNA strands, which is also important because the efficiency of non-homologous end joining was found to be different for guide RNAs complementary to the template and coding DNA strands [11].

The pX552_miCMV_Puro_SMN donor plasmid for homologous recombination in the *SMN2* gene was assembled as follows (Fig. 2a): sequences homologous to the regions flanking the DNA break (the so-called 5'- and 3'-homology arms) were placed on the outsides of the selection cassette carrying the puromycin resistance gene. The single-nucleotide T→C substitution was located in the 5'-homology arm, and the selection cassette was sup-

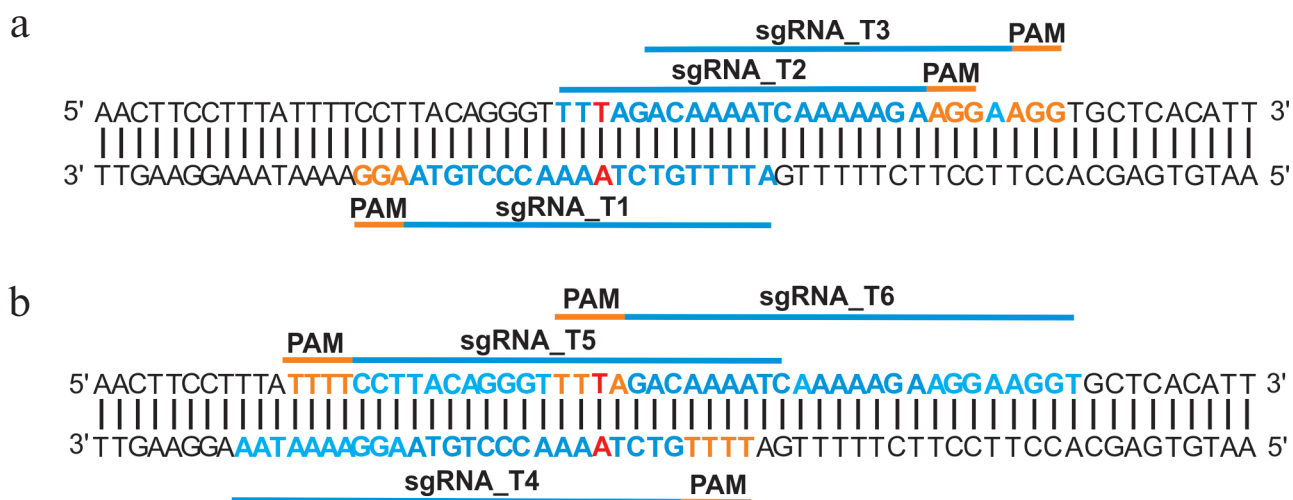


Fig. 1. Design of guide RNAs for exon 7 of the *SMN2* gene. a) Location of sgRNAs for CRISPR/Cas9. b) Location of sgRNAs for CRISPR/Cpf1. Single-nucleotide c.840C>T substitution in exon 7 of *SMN2* gene is shown in red; protospacer adjacent motifs (PAMs) required for the target recognition by CRISPR/Cas9 and CRISPR/Cpf1 are shown in orange.

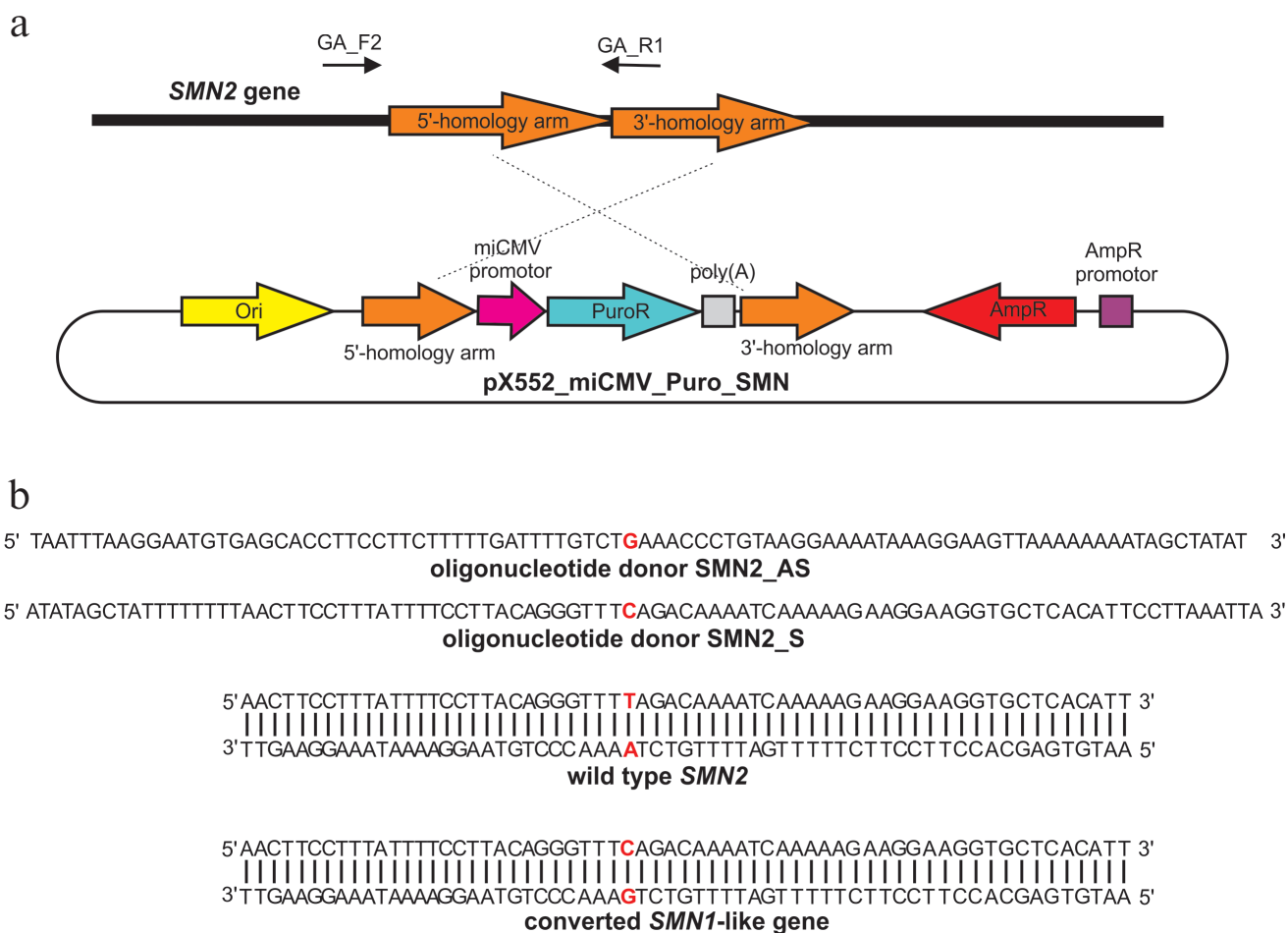


Fig. 2. a) Donor plasmid pX552_miCMV_Puro_SMN. GA_F2 and GA_R primers were used to verify insertion of the selection cassette. b) Single-stranded oligonucleotide donors; c.840C>T substitution in exon 7 of the *SMN2* gene is highlighted in red.

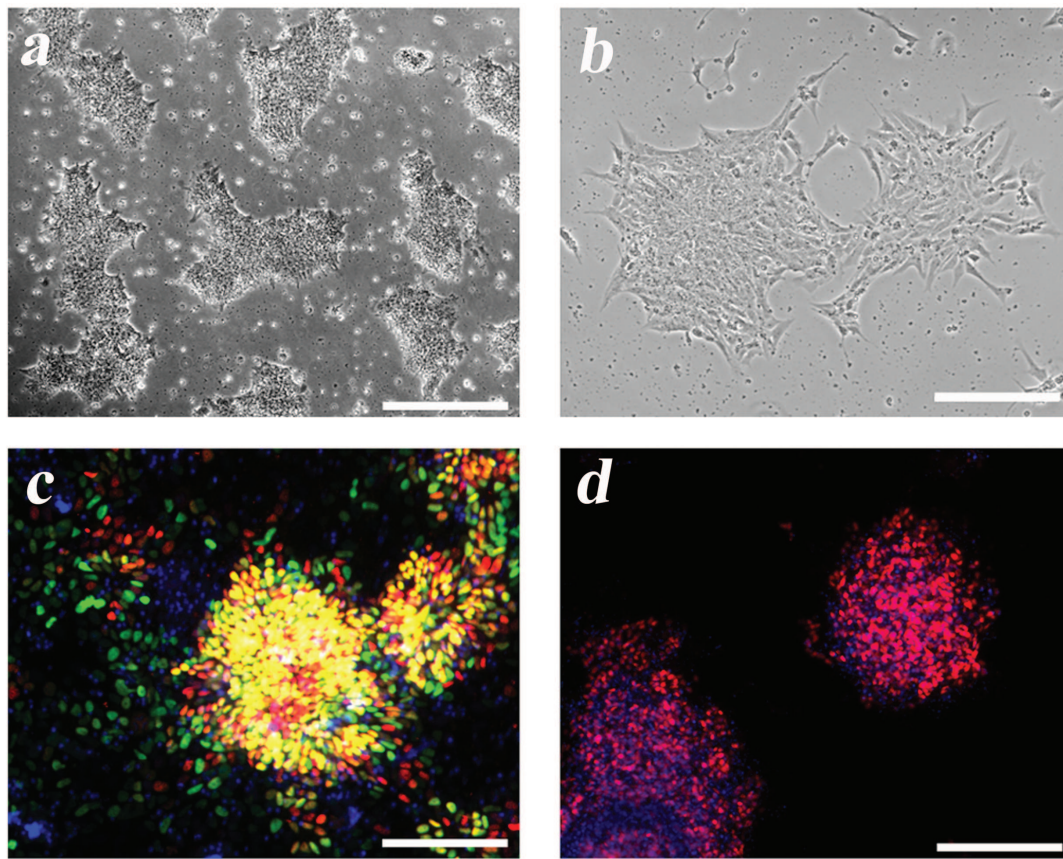


Fig. 3. Differentiation of iPSCs into MNPs. a) iPSC ICGi005-A on day 0 of differentiation. b) MNPs on day 12 of differentiation. c) Expression of neuroepithelial precursor markers PAX6 (red) and SOX1 (green) on day 6 of differentiation. d) Expression of the MNP marker OLIG2 (red) on day 12 of differentiation. Nuclei are stained with DAPI (blue). Scale bar, 200 μ m.

posed to integrate in intron 7 of *SMN2* gene after recombination. To prevent re-recognition and re-cutting by CRISPR/Cas9, additional synonymous single-nucleotide substitutions for the sgRNA_T1, sgRNA_T2, and sgRNA_T3 protospacers were introduced in the area immediately adjacent to PAM (protospacer 3'-region, "seed region"). When possible, codon usage frequencies were taken into account. Thus, the following additional substitutions were introduced into the 5'-homology arm in addition to the target T→C substitution:

– for T1: TCC→AGC (Ser; codon usage frequency, 17.7 and 19.4, respectively) and TTA→CTA (Leu; codon usage frequency, 7.6 and 7.1, respectively);

– for T2: AAA→AAG (Lys; codon usage frequency, 24.2 and 32.0, respectively) and CAA→CAG (Gln; codon usage frequency, 12.1 and 34.2, respectively);

– for T3: CGA→AGA (Arg; codon usage frequency, 6.2 and 11.9, respectively) and GGA→GGG (Gly; codon usage frequency, 16.4 and 16.5, respectively).

The amplified fragments were cloned into the plasmid vector; the length of the homology arms was ~500 bp (the optimal length for homologous recombination according to the published data [8]).

The following parameters were used for the design of oligonucleotide donors: 90-nt single-stranded oligonucleotides complementary to either the template (SMN1_S) or the coding (SMN1_AS) DNA strand. The T→C substitution was located approximately in the center of the donor oligonucleotide (Fig. 2b).

Generation of MNPs. Differentiation of ICGi005-A iPSCs (Fig. 3a) towards MNPs (Fig. 3b) was accompanied by the reduction in the expression of the *NANOG* gene (one of the main markers of pluripotent stem cells). At the same time, expression of the *PAX6* gene (neuroepithelial cell marker) increased on days 6 and 12 of differentiation and expression of the *OLIG2* gene (coding for the MNP transcription factor) increased on days 12 and 18 of differentiation (Fig. 4). On day 18, *PAX6* expression decreased, which can be explained by the fact that by this time, most of the neuroepithelial cells reached the stage of MNPs, as evidenced by a more than a 500-fold increase in the *OLIG2* expression. Immunocytochemical analysis confirmed expression of the major neuroepithelial markers PAX6 and SOX1, as well as the MNP marker OLIG2 (Fig. 3, c and d).

The advantage of MNPs is that these cells can be cultured for 10 passages or more without losing high pro-

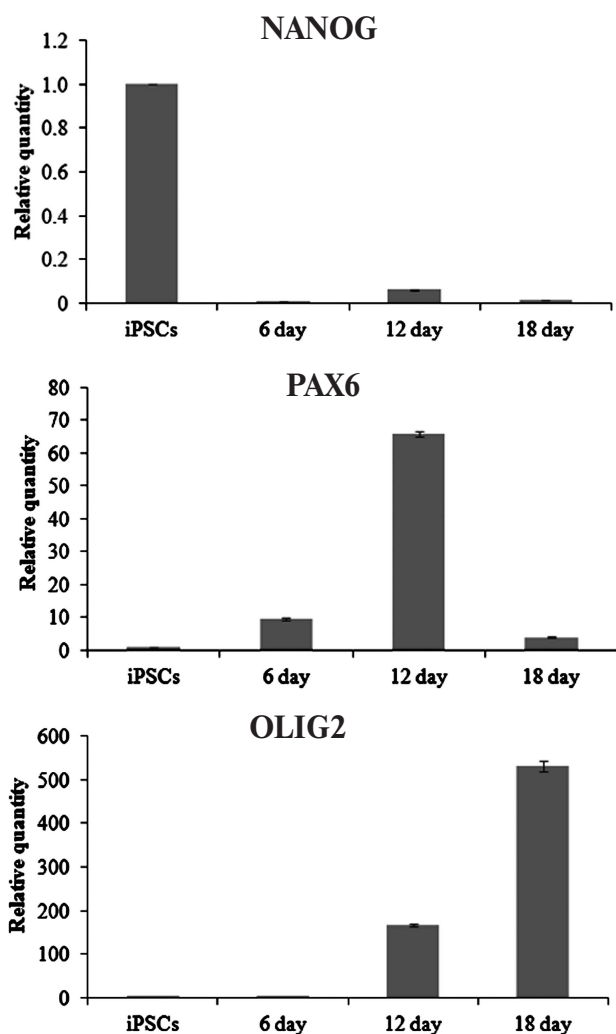


Fig. 4. Expression of *NANOG*, *PAX6*, and *OLIG2* during iPSC differentiation into MNPs.

liferative activity, *OLIG2* expression, and therefore, the ability to further differentiate toward mature motor neurons, which are the major type of cells suffering in SMA.

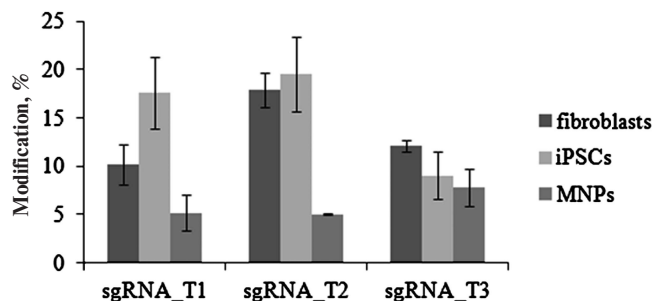
Comparative evaluation of the *SMN2* gene editing efficiency by CRISPR-mediated systems. To assess the efficiency of CRISPR/Cas9 in the *SMN2* gene editing, f1SMA fibroblasts from a patient with SMA type I, iPSCs ICGi005-A derived from the f1SMA fibroblasts, and MNPs obtained by differentiation of ICGi005-A cells were transfected with the pX458 plasmid expressing Cas9 protein, one of the guide RNAs (sgRNA_T1, sgRNA_T2, or sgRNA_T3), and GFP (green fluorescent protein).

The repair of double-strand DNA breaks by the non-homologous end joining generates small insertions and deletions, the number of which can be used to analyze the editing efficiency of a CRISPR system. One of the simplest and most reliable approaches for quantitative assessment of genome editing is the use of the TIDE web tool

for analysis of the sequencing patterns of PCR products obtained after delivery of the CRISPR system into the cells [12]. PCR products obtained from all experimental DNA samples were Sanger sequenced and analyzed using TIDE (Fig. 5). In fibroblasts, the editing activity of sgRNA_T2 was higher than the editing activities of sgRNA_T1 ($p < 0.05$) and sgRNA_T3 ($p < 0.05$). However, no significant differences in the editing efficiencies of all three guide RNAs were observed in the patient-specific iPSCs and MNPs. Comparison of the total CRISPR/Cas9 activity for the *SMN2* gene exon 7 in different cell types showed that the editing efficiency was higher in fibroblasts and iPSCs than in MNPs ($p < 0.05$). The highest CRISPR/Cas9 activity in fibroblasts, iPSCs, and MNPs was found with the sgRNA_T2 (trend at $p = 0.097$).

To assess the editing efficiency of the CRISPR/Cpf1 system in iPSCs ICGi005-A and MNPs, the cells were transfected with the pY010 plasmid expressing Cpf1 protein and the pTE4560 plasmid expressing one of the guide RNAs (sgRNA_T4, sgRNA_T5, sgRNA_T6) and mCherry red fluorescent protein. We found no significant differences in the editing efficiencies of sgRNA_T4, sgRNA_T5, and sgRNA_T6 in iPSCs and MNPs. However, the editing efficiency of CRISPR/Cpf1 was higher in iPSCs than in MNPs ($p < 0.05$).

Editing efficiency of CRISPR/Cas9 in exon 7 of *SMN2*



Editing efficiency of CRISPR/Cpf1 in exon 7 of *SMN2*

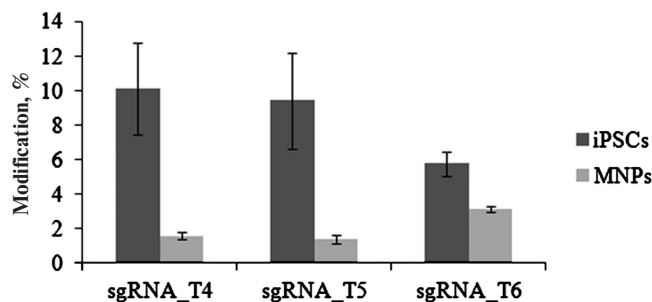


Fig. 5. Editing efficiency of CRISPR/Cas9 and CRISPR/Cpf1 in the *SMN2* gene exon 7 as analyzed by TIDE.

Comparative evaluation of the off-target activity of selected protospacers. To identify protospacers with the smallest number of off-target sites in the genome, we used bioinformatic analysis. Modern bioinformatic tools for identification of potential off-target sites for CRISPR/Cas9 use different algorithms. Comparison of these algorithms revealed that, although the protospacers suggested by different tools for a given genome region are the same, the number of identified potential off-target sites may vary [13]. It should be also noted that most of these tools reveal off-target sites containing single nucleotide substitutions relative to the target site; however, several studies have shown that off-target double-strand breaks can occur in sites containing insertions or deletions [14, 15]. Hence, we used several currently available bioinformatic tools to identify potential off-target sites: Cas-OFFinder and COSMID. The sequences of sgRNA_T1, sgRNA_T2, sgRNA_T3, sgRNA_T4, sgRNA_T5, and sgRNA_T6 protospacers, as well as complete human genome, were used as the input information.

Each algorithm identifies off-target sites containing nucleotide substitutions, insertions, and deletions relative to the sequence of the analyzed protospacer; however, Cas-OFFinder shows a total number of off-target sites without ranking the substitutions according to the probability of their occurrence. It is known that CRISPR/Cas9 most likely binds to the sites with substitutions located in the protospacer 5'-region, while substitutions in the 3'-region prevent the recognition of the DNA segment as a potential target [16]. Cas-OFFinder is more suitable for quick identification and comparison of the total number of off-target sites and substitutions in them. It also allows to evaluate the specificity of the selected CRISPR/Cas9 protospacers [13]. Using this tool, we determined the total number of off-target sites with the minimal number of replacements equal to 3: 24, 72 and 115 off-target sites for sgRNA_T1, sgRNA_T2, and sgRNA_T3, respectively. Therefore, it seemed more reliable to use sgRNA_T1, because the total number of

off-target sites for this protospacer was less than for sgRNA_T2 and sgRNA_T3.

COSMID assigns a rank to each off-target site – the lower the rank, the higher the probability of the off-target effect (the target site has a rank of 0.00). After analysis, we obtained a list of the most likely off-target sites containing no more than four substitutions and/or insertions/deletions of no more than 2 nt. The smallest number of the off-target sites was found for sgRNA_T1, the largest – for sgRNA_T3. However, the majority of potential off-target sites for CRISPR/Cas9 had a very high rank and were located in the non-coding regions and intergenic gaps. Therefore, only those sites that were located in the coding regions were selected from the obtained list (Table 2). Then, we analyze the activity of CRISPR/Cas9 at these sites in fibroblasts, iPSCs, and MNPs using TIDE (as described above). As a result, no insertions/deletions were detected in these DNA sites.

Similar analysis was carried out to assess potential off-target activity of CRISPR/Cpf1, which was found to be significantly lower than that of CRISPR/Cas9, since the guide RNA for CRISPR/Cpf1 is longer. Using the Cas-OFFinder software, three potential off-target sites were found for sgRNA_T4, 0 sites – for sgRNA_T5, and 5 sites – for sgRNA_T6. No off-target sites were found in genome coding regions; hence, no experimental assessment of the CRISPR/Cpf1 off-target activity in the most probable genome sites was performed.

Therefore, all tested protospacers for the CRISPR/Cpf1 system and sgRNA_T1 and sgRNA_T2 for CRISPR/Cas9 were found to be optimal in terms of potential off-target activity.

Evaluation of the efficiency of the CRISPR-mediated systems in the correction of the single-nucleotide c.840C>T substitution in exon 7 of the SMN2 gene. In order to evaluate the efficiency of the editing system to make the single-nucleotide T>C substitution in exon 7 of the SMN2 gene, f1SMA fibroblasts were transfected with the pX458 plasmid expressing Cas9 and sgRNA_T2 and the donor plasmid pX552_miCMV_Puro_SMN1. Forty-

Table 2. Off-target sites for CRISPR/Cas9 in genome coding regions

Protospacer	Gene	Location	PAM	Sequence
sgRNA_T1	<i>LOC105376917</i>	chr19:–22494728	GAG	AATATGTTTAAACCCTGTA
	<i>PRPS2</i>	chrX:+12823219	TAG	CATTGGGTAAAACCCTGTA
sgRNA_T2	<i>FANCD2</i>	chr3:+10072949	AAG	TTCAGCAAAAATCAGAAAGA
	<i>FANCD2P2</i>	chr3:+11891166	GAG	TTCAGCAAAAATCAGAAAGA
sgRNA_T3	<i>LOC105369801</i>	chr12:+64010927	AAG	TATAAAATCAAAAGGAAGGA
	<i>LIN28B</i>	chr6:+104957098	AAG	AAAAAATCAAAAGGAAGGA

Note: Substitutions in the off-target sites are highlighted in grey.

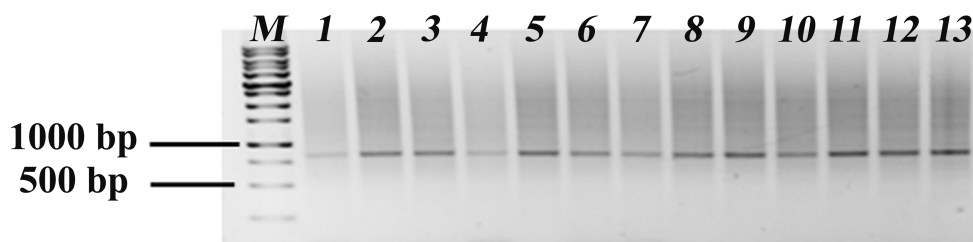


Fig. 6. PCR analysis for the presence of selection cassette. Lanes: *M*) markers; *1*) mixed population of f1SMA fibroblasts; *2*) mixed population of iPSCs ICGi005-A; *3-13*) individual iPSC ICGi005-A clones.

eight hours after transfection, GFP-positive (and therefore, expressing components of the CRISPR/Cas9 system) cells were selected using a cell sorter. Forty-eight hours after this procedure, puromycin was added to the culture medium at a concentration of 850 ng/ml for 4 days to select recombinant cells with the integrated selection cassette, i.e., cell that underwent homologous recombination. Insertion of the selection cassette was verified by PCR: in the case of insertion, the product of PCR with the primers, one of which was complementary to the sequence outside the 5'-homology arm and the other one – to the sequence within the 3'-homology arm, should be longer by the size of the selection cassette (1664 vs. 850 bp). However, PCR analysis of the mixed cell population obtained after selection revealed only the 850-bp (wild-type) products (Fig. 6). TIDE analysis of these products demonstrated that the editing efficiency was 27.7% (as estimated from the number of insertions/deletions).

Taking into account the obtained data, similar experiment was carried out in iPSCs ICGi005-A. In this case, selection was performed in two rounds using puromycin concentration of 250 ng/ml. The resulting subclones and mixed cell population were analyzed separately. According to the PCR of mixed cell population and individual clones obtained by selection, only wild-type products were detected (Fig. 6). TIDE analysis of the mixed population showed that the editing efficiency was 23%.

Because of ambiguous results obtained in the experiments with the plasmid donor, we decided to use single-stranded oligonucleotide donors containing the target single-nucleotide substitution. Analogous experiment was carried out using a vector expressing sgRNA_T1 and SMN_AS/SMN_S oligonucleotides. According to TIDER (modified version of TIDE), the average number of T>C substitutions in the target locus with the SMN_S oligonucleotide was $13.7 \pm 1.7\%$; the number of targeted substitutions with the SMN_AS antisense sequence of the donor oligonucleotide was $15.25 \pm 0.35\%$. Comparable editing efficiency values were obtained in a similar experiment with MNPs: $15.9 \pm 2.40\%$ for the sense sequence and $16.35 \pm 1.34\%$ for the antisense sequence.

DISCUSSION

In this work, we analyzed the activity of CRISPR/Cas9 and CRISPR/Cpf1 in exon 7 of the *SMN2* gene in fibroblasts, iPSCs, and MNPs obtained from a patient with SMA. Despite the fact that sgRNA_T1 and sgRNA_T2/sgRNA_T3 were complementary to the template and coding DNA strands, respectively, significant differences in their editing efficiency were found only in the fibroblasts. No significant differences in the repair efficiency by the non-homologous end joining with different guide RNAs were observed in iPSCs and MNPs, which are of most interest as precursors of motor neurons. However, comparison of the editing efficiency of CRISPR/Cas9 and CRISPR/Cpf1 in different cell types showed that the editing efficiency in MNPs was significantly lower than in iPSCs. In all likelihood, this might be explained by the specific properties of these cells or by the non-optimal delivery of the plasmid construct to MNPs.

Evaluation of potential off-target sites showed that sgRNA_T3 had the greatest risk of the off-target effects: the genome contains two sites in the *LIN28B* and *LOC105369801* genes that differ only by three bases from the target sequence, with two bases located in the 5'-region of the protospacer. For sgRNA_T1 and sgRNA_T2, the probability of damage to the coding regions is rather low, which was experimentally confirmed. In the case of CRISPR/Cpf1 system, the probability of the off-target site damage was much lower. In addition, reduction of off-target activity can be achieved by introducing modified variants of Cas9, as well as using short-lived RNA–protein complexes of sgRNA-Cas9 instead of plasmid vectors [8].

Since application of human genome editing tools is related to personalized medicine, selection of potential targets for CRISPR/Cas9 should take into account genetic polymorphisms. Analysis of the protospacers used in this work with the CRISPOR resource (<http://crispor.tefor.net/>) and the hg19 version of human genome found that one of the polymorphisms (G substitution with C) eliminates PAM adjacent to the most efficient protospacer sgRNA_T2 and, being located in the critical region,

most likely makes sgRNA_T3 inactive. The occurrence frequency of this polymorphism is ~1%. Therefore, only sgRNA_T1 can be used in this case for correction of the c.840C>T substitutions.

The use of plasmid donor for correction of the single-nucleotide c.840C>T substitution in exon 7 of the *SMN2* gene demonstrated a high probability of off-target insertions with the low probability of target insertions, which might be related to the circular shape of the plasmid molecule. A number of studies have demonstrated a higher efficiency of linearized plasmid donors containing only homology arms and selection cassette and lacking other elements of the donor plasmid [17]. However, we found that the use of single-stranded oligonucleotide donors ensures efficient introduction of the target T>C substitution into exon 7 of the *SMN2* gene in iPSC and MNPs, which is consistent with the evidence that short oligonucleotide donors are preferable for recombination aimed to introduce single-nucleotide substitutions [8].

Funding. This work was supported by the Russian Science Foundation (project 17-75-10041).

Acknowledgements. The authors are grateful to A. A. Nemudryi for help in assembling pX552_miCMV_Puro_SMN.

Conflict of interest. The authors declare no conflict of interest.

Ethical approval. All procedures performed in studies involving human participants were in accordance with the ethical standards of the institutional and/or national research committee and with the 1964 Helsinki declaration and its later amendments or comparable ethical standards.

REFERENCES

1. Verhaart, I. E., Robertson, A., Leary, R., McMacken, G., König, K., Kirschner, J., Jones, C. C., Cook, S. F., and Lochmüller, H. (2017) A multi-source approach to determine SMA incidence and research ready population, *J. Neurol.*, **264**, 1465-1473, doi: 10.1007/s00415-017-8549-1.
2. Lefebvre, S., Burglen, L., Reboullet, S., Clermont, O., Burlet, P., Viollet, L., Benichou, B., Cruaud, C., Millasseau, P., Zeviani, M., Le Paslier, D., Frezal, J., Cohen, D., Weissenbach, J., Munnich, A., and Melki, J. (1995) Identification and characterization of a spinal muscular atrophy-determining gene, *Cell*, **80**, 155-165, doi: 0092-8674(95)90460-3.
3. Monani, U. R., Lorson, C. L., Parsons, D. W., Prior, T. W., Androphy, E. J., Burghes, A. H., and McPherson, J. D. (1999) A single nucleotide difference that alters splicing patterns distinguishes the SMA gene *SMN1* from the copy gene *SMN2*, *Hum. Mol. Genet.*, **8**, 1177-1183.
4. Cartegni, L., and Krainer, A. R. (2002) Disruption of an SF2/ASF-dependent exonic splicing enhancer in *SMN2* causes spinal muscular atrophy in the absence of *SMN1*, *Nat. Genet.*, **30**, 377-384, doi: 10.1038/ng854.
5. Kashima, T., and Manley, J. L. (2003) A negative element in *SMN2* exon 7 inhibits splicing in spinal muscular atrophy, *Nat. Genet.*, **34**, 460-463, doi: 10.1038/ng1207.
6. McAndrew, P. E., Parsons, D. W., Simard, L. R., Rochette, C., Ray, P. N., Mendell, J. R., Prior, T. W., and Burghes, A. H. (1997) Identification of proximal spinal muscular atrophy carriers and patients by analysis of *SMN1* and *SMN2* gene copy number, *Am. J. Hum. Genet.*, **60**, 1411-1422, doi: 10.1086/515465.
7. Gidaro, T., and Servais, L. (2019) Nusinersen treatment of spinal muscular atrophy: current knowledge and existing gaps, *Dev. Med. Child Neurol.*, **61**, 19-24, doi: 10.1111/dmcn.14027.
8. Liang, X., Potter, J., Kumar, S., Ravinder, N., and Chesnut, J. D. (2017) Enhanced CRISPR/Cas9-mediated precise genome editing by improved design and delivery of gRNA, Cas9 nuclease, and donor DNA, *J. Biotechnol.*, **241**, 136-146, doi: 10.1016/j.jbiotec.2016.11.011.
9. Valetdinova, K. R., Maretina, M. A., Kuranova, M. L., Grigor'eva, E. V., Minina, Y. M., Kizilova, E. A., Kiselev, A. V., Medvedev, S. P., Baranov, V. S., and Zakian, S. M. (2019) Generation of two spinal muscular atrophy (SMA) type I patient-derived induced pluripotent stem cell (iPSC) lines and two SMA type II patient-derived iPSC lines, *Stem Cell Res.*, **34**, 101376, doi: 10.1016/j.scr.2018.101376.
10. Du, Z. W., Chen, H., Liu, H., Lu, J., Qian, K., Huang, C. L., Zhong, X., Fan, F., and Zhang, S. C. (2015) Generation and expansion of highly pure motor neuron progenitors from human pluripotent stem cells, *Nat. Commun.*, **6**, 6626, doi: 10.1038/ncomms7626.
11. Clarke, R., Heler, R., MacDougall, M. S., Yeo, N. C., Chavez, A., Regan, M., Hanakahi, L., Church, G. M., Marraffini, L. A., and Merrill, B. (2018) Enhanced bacterial immunity and mammalian genome editing via RNA-polymerase-mediated dislodging of Cas9 from double strand DNA breaks, *Mol. Cell*, **71**, 42-55, doi: 10.1016/j.molcel.2018.06.005.
12. Brinkman, E. K., Chen, T., Amendola, M., and van Steensel, B. (2014) Easy quantitative assessment of genome editing by sequence trace decomposition, *Nucleic Acids Res.*, **42**, e168, doi: 10.1093/nar/gku936.
13. Ishida, K., Gee, P., and Hotta, A. (2015) Minimizing off-target mutagenesis risks caused by programmable nucleases, *Int. J. Mol. Sci.*, **16**, 24751-24771, doi: 10.3390/ijms161024751.
14. Ran, F. A., Cong, L., Yan, W. X., Scott, D. A., Gootenberg, J. S., Kriz, A. J., Zetsche, B., Shalem, O., Wu, X., Makarova, K. S., Koonin, E. V., Sharp, P. A., and Zhang, F. (2015) *In vivo* genome editing using *Staphylococcus aureus* Cas9, *Nature*, **520**, 186-191, doi: 10.1038/nature14299.
15. Lin, Y., Cradick, T. J., Brown, M. T., Deshmukh, H., Ranjan, P., Sarode, N., Wile, B. M., Vertino, P. M., Stewart, F. J., and Bao, G. (2014) CRISPR/Cas9 systems have off-target activity with insertions or deletions between target DNA and guide RNA sequences, *Nucleic Acids Res.*, **42**, 7473-7485, doi: 10.1093/nar/gku402.
16. Nemudryi, A. A., Valetdinova, K. R., Medvedev, S. P., and Zakian, S. M. (2014) TALEN and CRISPR/Cas genome editing systems: tools of discovery, *Acta Naturae*, **6**, 19-40.
17. Song, F., and Stieger, K. (2017) Optimizing the DNA donor template for homology-directed repair of double-strand breaks, *Mol. Ther. Nucleic Acids*, **7**, 53-60, doi: 10.1016/j.omtn.2017.02.006.